Navier-Stokes Analysis of Flow and Heat Transfer Inside High-Pressure-Ratio Transonic Turbine Blade Rows

C. Hah*
NASA Lewis Research Center, Cleveland, Ohio 44135
and
R. J. Selva†
Cray Research, Inc., Mendota Heights, Minnesota 55120

A detailed numerical study of the flow and the heat transfer inside high-pressure-ratio transonic/supersonic turbine blade rows is described. A high-order upwinding relaxation method is used to solve the Reynolds-averaged Navier-Stokes equation inside three different turbine blade rows. A two-equation turbulence model with a low-Reynolds-number modification is used to describe turbulent shear stress and turbulent heat flux. The numerical results are compared with available experimental data on two-dimensional geometries. It is found that very complex flow phenomena near the trailing edge of transonic turbine blade rows can be very well predicted numerically, and the method can be used in the development of new designs for HP turbines.

Nomenclature

C_1, C_2, C_3, C_4, C_μ, σ_{dk}, σ_ε = constants in turbulence closure models
C_m = total relative velocity
C_v = specific heat
F_i = additional body force in equation 2
H = heat transfer coefficient
k = turbulence kinetic energy
k_c = thermal conductivity
l = distance from wall
P = $-\overline{u_i u_j} U_{ij}$
p = static pressure
R = gas constant
u_* = friction velocity
β = coefficient of thermal expansion
δ_{ij} = Kronecker delta
ε_{ijk} = permutation tensor
ν = kinematic viscosity
ρ = density
Ω_i = angular velocity of impeller

Subscripts

t = total
w = value at wall
∞ = upstream condition
2 = downstream condition

Superscript

$-$ = average value

Introduction

EFFICIENT turbomachinery blades traditionally have been developed through the systematic testing of blade profiles in cascade wind tunnels. With the recent introduction of a numerical method that can correctly predict both pressure field and aerodynamic losses, development of new blade sections relies increasingly on numerical analysis rather than on direct experimental tests.

Although various numerical methods, such as streamline curvature, potential flow, Euler, and Euler plus boundary layer coupling, are extensively used in the design process of new turbomachinery stages, Navier-Stokes methods are frequently used to get more detailed and realistic pictures of the flow, and various previous numerical studies based on Navier-Stokes solutions[1-4] have shown great promise in component design applications. These calculations model boundary layer development, horseshoe and passage vortex flow, and wake development very well, especially for subsonic flows in turbines and compressors.

However, many jet engine turbines operate with transonic and supersonic flow to obtain a high pressure ratio across the blade row. In high-pressure-ratio turbine flow, shock, and shock-boundary layer interaction cause a significant portion of the aerodynamic loss, in addition to the traditional losses from boundary layer, wake mixing, and secondary flows.

The flow inside a high-pressure-ratio turbine blade row is extremely complex. The flow transition occurs on both the suction side and the pressure side of the blade. The flow at the trailing edge is supersonic and a very complex shock system is developed near the trailing edge. The general structure of the flow is illustrated in Fig. 1. The pressure-side shock propagates toward the suction surface of the adjacent blade and interacts with the blade boundary layer. The other shock, which is usually much stronger, runs downstream away from the blades and interacts with the blade rows that follow. Although the basic physics of the flow is fairly well understood,[5,6] the reliable prediction of this flow has been extremely difficult.

The purpose of this study was to develop and evaluate a numerical method to predict the viscous flow inside high-pressure-ratio transonic turbine blade rows. A modified two-equation turbulence model with a low-Reynolds-number correction is used to describe flow transition, turbulence stress, and heat flux. A pressure-based relaxation method with a third-order accurate upwinding is used to solve the governing equations and the turbulence transport equation.[7]

The current method is applied to predict flow and heat transfer inside various HP turbine blade rows at typical operating conditions. The numerical results are evaluated with well-documented experimental data.

Presented as Paper 90-0343 at the AIAA 28th Aerospace Sciences Meeting, Reno, NV, Jan. 8–11, 1990; received March 15, 1990; revision received Nov. 15, 1990; accepted for publication Dec. 4, 1990.

*Senior Scientist, Internal Fluid Mechanics Division; formerly, Staff Engineer, R & D Center, General Electric Company. Member AIAA.
†Senior Sales Analyst.

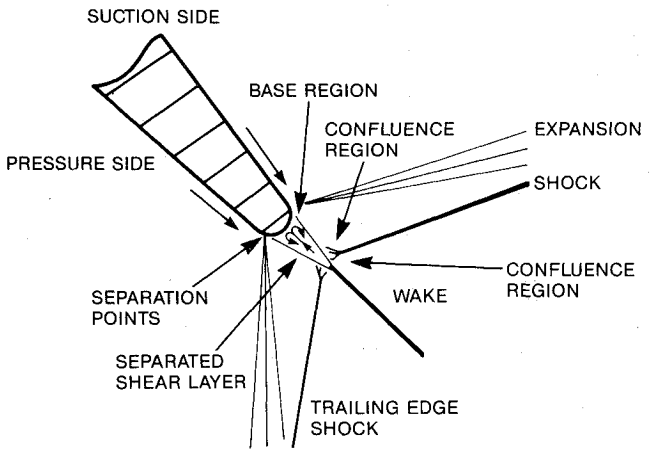

Fig. 1 Flow structure near the trailing edge of HP turbine blade.

This study evaluates the current status of the numerical technique used in designing a high-pressure-ratio turbine blade section. Areas of further development and possible direct application of the design code are also discussed.

Governing Equations and Turbulence Modeling

The following Reynolds-averaged Navier-Stokes equations are solved for the current problem

$$\frac{\partial}{\partial x_i}(\rho U_i) = 0 \tag{1}$$

$$\frac{\partial}{\partial x_j}(\rho U_i U_j) + 2\rho\varepsilon_{ijk}\Omega_j U_K = \frac{\partial p}{\partial x_i} + \frac{\partial}{\partial x_j}\left[\mu\left(\frac{\partial U_i}{\partial x_j} + \frac{\partial U_j}{\partial x_i} - \frac{2}{3}\frac{\partial U_k}{\partial x_k}\delta_{ij}\right) - \rho\overline{u_i u_j}\right] + F_i \tag{2}$$

$$\frac{\partial}{\partial x_j}(\rho U_j e) = \frac{\partial}{\partial x_j}\left[\left(\frac{\mu}{Pr}\right)_{\text{eff}}\frac{\partial T}{\partial x_j}\right] - \frac{\partial}{\partial x_j}(pU_j) + U_i F_i + \frac{\partial}{\partial x_j}\left[U_i\mu\left(\frac{\partial U_i}{\partial x_j} + \frac{\partial U_j}{\partial x_i} - \frac{2}{3}\frac{\partial U_k}{\partial x_k}\delta_{ij}\right)\right] \tag{3}$$

$$p = \rho RT \tag{4}$$

where U_i = mean velocity, u_i = fluctuating velocity, e = total energy, Ω_i = angular velocity,

$$\left(\frac{\mu}{Pr}\right)_{\text{eff}} = \left(\frac{\mu}{Pr}\right)_{\text{laminar}} + \left(\frac{\mu}{Pr}\right)_{\text{turbulent}}$$

and

$$e = C_v T + \frac{1}{2}U_i U_i$$

A modified two-equation k-ε model is used to estimate Reynolds stresses and heat flux. The turbulence model is extended to the solid wall following the studies of Chien.[8] Evaluation of various turbulence models for the computation of the transonic turbine flow is not the object of the current work. Rather, a well-established model with proper modification for the near wall effects is used. Also, the current turbulence model is known to predict flow transition when the transition is caused primarily by free stream turbulence. Consequently, the numerical solution was started with the laminar boundary layer profile over the entire blade surface. During the numerical solution, turbulence kinetic energy is convected from the free stream toward the blade surface boundary layer. Laminar to turbulent boundary layer transition is obtained on the blade surface, where sufficient turbulence kinetic energy is transported with the current turbulence modeling equations. The following additional transport equations are solved to calculate turbulent stress terms

$$\frac{\partial(\rho U_i k)}{\partial x_i} = \frac{\partial}{\partial x_i}\left(\frac{\mu_{\text{eff}}}{\sigma_k}\frac{\partial k}{\partial x_i}\right) - \rho\overline{u_i u_j}U_{i,j} - \rho\varepsilon - \frac{2\mu k}{l^2} \tag{5}$$

$$\frac{\partial(\rho U_i \varepsilon)}{\partial x_i} = \frac{\partial}{\partial x_i}\left(\frac{\mu_{\text{eff}}}{\sigma_\varepsilon}\frac{\partial \varepsilon}{\partial x_i}\right) + C_1\frac{\rho\varepsilon}{k}(\overline{u_i u_j}U_{i,j}) - \frac{\rho\varepsilon}{k}\left(C_2 f\varepsilon + \frac{2\nu k e^{-C_3 u^* l/\nu}}{l^2}\right) \tag{6}$$

where

$$\mu_{\text{eff}} = \mu + C_\mu\rho(k^2/\varepsilon)\,[1 - e^{-C_3 u^* l/\nu}]$$

and

$$f = 1 - \frac{0.4}{1.8}e^{-(k_2/6\nu\varepsilon)^2}$$

No attempt was made to optimize constants of the turbulence modeling equations for this study. Therefore, standard values of various constants of the turbulence model are used; the values are

$$C_\mu = 0.09,\ C_1 = 1.35,\ C_2 = 1.8,\ \sigma_k = 1.0,\ \sigma_\varepsilon = 1.3$$

$$C_3 = 0.0115,\ C_4 = 0.5$$

Numerical Scheme and Boundary Conditions

Equations (1–6) are solved numerically with a fully conservative control volume approach. The finite difference equations are formulated in terms of Cartesian momentum (ρU_i), static pressure (p), total internal energy (e), turbulence kinetic energy (k), and turbulence energy dissipation rate (ε). The numerical fluxes through control volume surfaces are estimated with a quadratic upwinding scheme and so the formal spatial accuracy is third order on smoothly varying meshes. The steady-state solution is obtained through the elliptic relaxation of the finite difference equations and each relaxation consists of one semi-implicit prediction and two implicit correction steps. During each iteration, pressure-based correction equations are used to ensure global conservation.

With the static pressure field at the previous iteration, the momentum conservation equations are solved using the following equation on nonorthogonal body-fitted coordinates:

$$\frac{1}{J}\frac{\partial}{\partial\xi}(G_1\phi) + \frac{1}{J}\frac{\partial}{\partial\eta}(G_2\phi) + \frac{1}{J}\frac{\partial}{\partial\psi}(G_3\phi) = \frac{1}{J}\frac{\partial}{\partial\xi}\left[\frac{\Gamma'_\phi}{J}D_{\xi\xi}\phi_\xi + \frac{\Gamma'_\phi}{J}D_{\xi\eta}\phi_\eta + \frac{\Gamma'_\phi}{J}D_{\xi\psi}\phi_\psi\right] + \frac{1}{J}\frac{\partial}{\partial\eta}\left[\frac{\Gamma'_\phi}{J}D_{\eta\xi}\phi_\xi + \frac{\Gamma'_\phi}{J}D_{\eta\eta}\phi_\eta + \frac{\Gamma'_\phi}{J}D_{\eta\psi}\phi_\psi\right] + \frac{1}{J}\frac{\partial}{\partial\psi}\left[\frac{\Gamma'_\phi}{J}D_{\psi\xi}\phi_\xi + \frac{\Gamma'_\phi}{J}D_{\psi\eta}\phi_\eta + \frac{\Gamma'_\phi}{J}D_{\psi\psi}\phi_\psi\right] + \tilde{S}_\phi \tag{7}$$

Table 1 The key geometry and flow parameters

	Rotor cascade	RD turbine	VKI turbine
Pitch/chord	0.74	0.842	0.85
Stagger angle	35	29.6	55
L.E. radius/chord ratio	0.055	0.053	0.061
Downstream Mach number	1.2	1.2	1.05
Inlet total temperature	293 K	293 K	420 K
Blade surface temperature	Adiabatic	Adiabatic	293 K

where Γ'_ϕ is the diffusion coefficient, G_i is a velocity component along the transformed coordinates (ξ, η, ψ), and $\bar{S}_\phi$ consists of additional body force terms and pressure terms. A three-point central difference approximation is used for all the diffusion terms and a modified quadratic upwinding scheme is used for convection terms.

Because the coefficients of the finite difference representation of Eq. (7) are based on the values at the previous step, the resulting ρU_i does not satisfy mass conservation. Two correction steps are needed to satisfy the mass conservation at each iteration. The concept of pressure-implicit splitting is used for the correction of p and ρU_i after the prediction step.

The two correction steps are as follows:

$$(\rho U_i)^{**} - (\rho U_i)^{*} = \Delta_p^{-1} \Delta_i (p^{*} - p^{n}) \tag{8}$$

$$(\rho U_i)^{n+1} - (\rho U_i)^{**} = A_p^{-1} \Sigma A_{pm} [(\rho U)^{**} - (\rho U)^{*}] - \Delta_i (p^{n+1} - p^{*}) \tag{9}$$

For Eqs. (8) and (9), the mass conservation condition is imposed as

$$\Delta_i (\rho U_i)^{**} = \Delta_i (\rho U_i)^{n+1} = \Delta_i (\rho U_i)^{**} = 0 \tag{10}$$

By combining Eq. (10) with Eqs. (8) and (9), Poisson-type equations are obtained for $(p^{*} - p^{n})$ and $(p^{**} - p^{*})$ and the value of $(\rho U)_i^{n+1}$ and p^{n+1} is calculated with the corrected pressure. With the correction step in Eqs. (8)–(10), density is handled rather implicitly and ρU_i and p are updated. A single implicit step is used to calculate k, ε, and e with the corrected values of ρU_i and p.

The computations were carried out on I-O type composite grids. With the I-grid, spatial periodicity of the grid at the periodicity surface is not forced and the physical flow periodicity condition is handled inside the flow solver by a high-order interpolation of variables. To satisfy the periodicity condition of the flowfield between periodicity surfaces, a second-order interpolation of flow variable is used on each periodicity surface. As the strict numerical interpolation of flow variables does not ensure conservation of flow properties across these surfaces, the mean values of the flow properties are readjusted to enforce the overall conservation. Good orthogonality of the grid can be maintained near the blade surface and at periodic surfaces, which is essential for the accurate solution of transonic viscous flow inside turbine blade rows with high turning. Near the blade surface, an O-grid is wrapped around the blade. This inner O-grid, which extends only 1–2% of the chord length from the blade surface toward the free stream, is used primarily to represent the high gradient of variables near the surface. Variables at the interface between I- and O-grids are interpolated with a second-order accurate function. With the I-O type grid, dimensionless wall distance (y^+) at the first node can be on the order of 1 to 5 with an acceptable overall grid size.

At the inflow boundary, the distribution of total pressure, total temperature, and inlet flow angles is fixed. At the outflow boundary, the static pressure is fixed at one location. For the turbulence, the experimental value of turbulent kinetic energy is used at the inflow boundary and the equilibrium condition is used to estimate the inflow condition of the turbulence dissipation rate. Residuals of each finite difference equation are integrated over the entire domain. When the integrated residuals of all the equations are reduced by four orders of magnitude from their initial value, the solution is considered to be converged. The code is vectorized on a Cray-XMP computer and has an option to run out-of-core solutions (solid-state disk storage on a Cray-XMP) for large-scale problems.

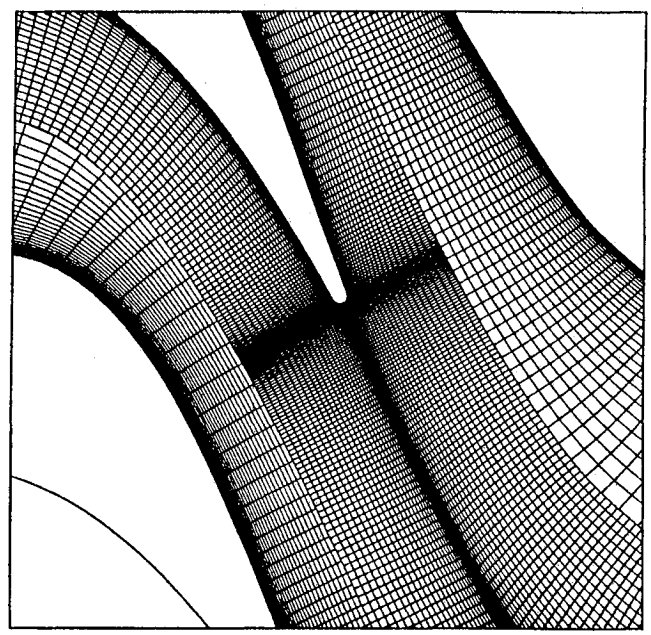

Fig. 2 Computational grid near the trailing edge.

Results and Discussion

The current numerical method using the k-ε turbulence model was evaluated to determine the transonic flows inside three high-pressure-ratio turbine blade sections. These turbine bladings are representative of modern design practice for the high-pressure-ratio turbines of various manufacturers.

As shown in Fig. 1, a complex shock system is developed near the trailing edge of the turbine blade when the exit Mach number is above 1.2. The strong shock on the suction side travels toward the next blade row and induces strong unsteady loading across the stage, which is thought to be detrimental to the aerodynamic performance. One of the goals of the advanced design of high-pressure-ratio turbine blading is to control or reduce this shock strength. Important geometry and flow parameters of the three turbine blade rows are given in Table 1.

Turbine Rotor Cascade

An experimental study to investigate the detailed flowfield of a turbine rotor section was conducted at GE. Detailed computational grids near the trailing edge of this cascade are shown in Fig. 2. This figure shows that a nearly orthogonal grid was obtained near the trailing edge, where a trailing edge shock system exists. The computation was performed using 20,400 nodes (164 nodes in the streamwise direction and 100 nodes in the blade-to-blade direction for the I-grid and 4000 nodes for the O-grid). The computed static pressure contours

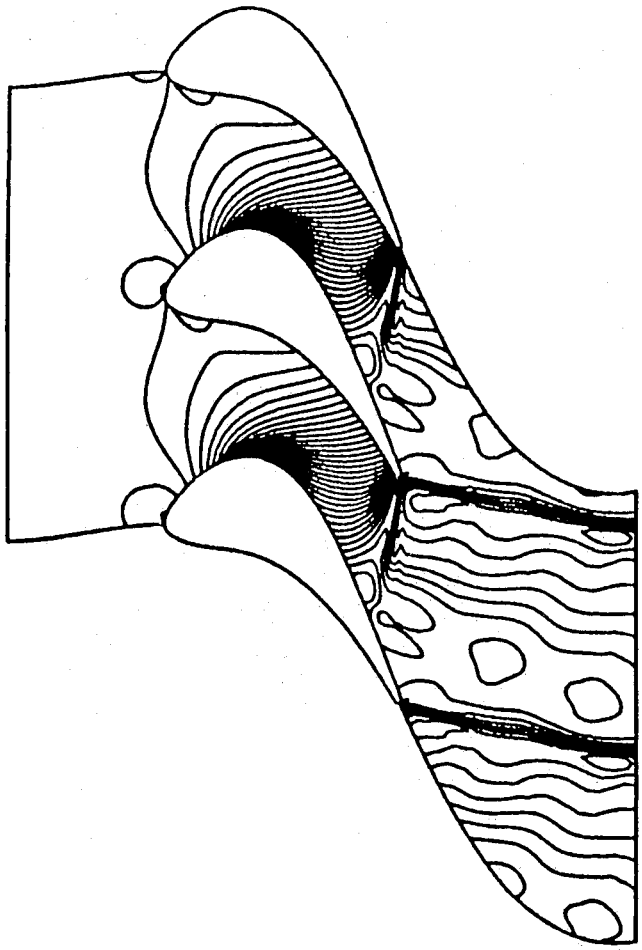

Fig. 3 Calculated static pressure contours.

are shown in Fig. 3 and details near the trailing edge region are given in Fig. 4. In Fig. 5, the calculated static pressure distribution on the blade surface is compared with the measured data. As shown in Figs. 3–5, respectively, the shock structure, trailing edge pressure field, and airfoil surface pressure distribution are accurately predicted.

The current method calculates the base pressure, a clear constant-pressure zone near the trailing edge (Fig. 4). Knowledge of the base pressure is of primary importance for calculating the trailing edge losses and the cooling-air flow. Because the details of the flowfield near the trailing edge are determined by the viscous stresses, it is believed that the base pressure cannot be calculated with potential or inviscid flow calculation methods. Detailed Mach number contours near the trailing edge are shown in Fig. 6. As shown in Fig. 6, the trailing edge shock system is detached from the actual trailing edge because of a small separation bubble near the trailing edge. Detailed velocity vectors near the trailing edge are shown in Fig. 7. The numerical results in Figs. 3–6 confirm that the current numerical method with the applied turbulence closure model correctly predicts the detailed flowfield inside the high-pressure-ratio turbine blade rows.

RD HP Turbine Blade

Calculations also have been performed for a high-pressure-ratio turbine rotor profile. The blade designated RD is typical of recent gas turbine design and has been used for numerical verification by various groups. The geometry of the blade section, which is from a high-work-capacity transonic turbine, is discussed in Ref. 10.

A total of 20,400 computational nodes is used for the solution. In Fig. 8, the calculated density contours are compared with measured data and with two previously published nu-

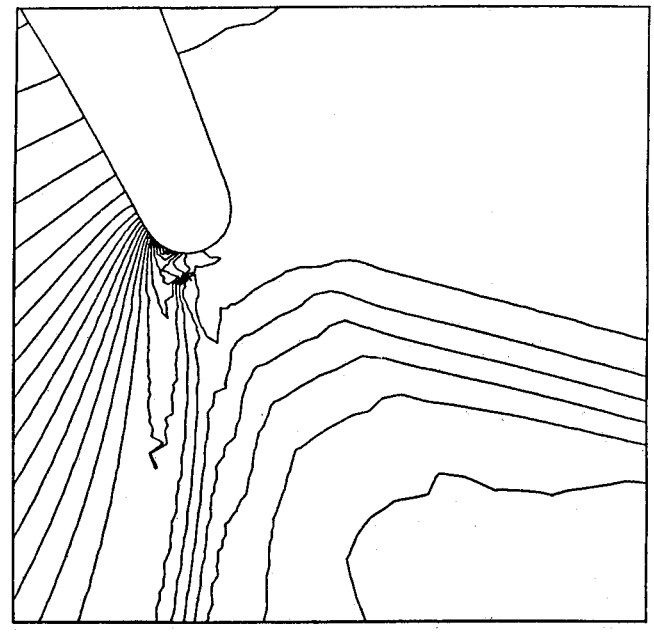

Fig. 4 Calculated static pressure contours near the trailing edge.

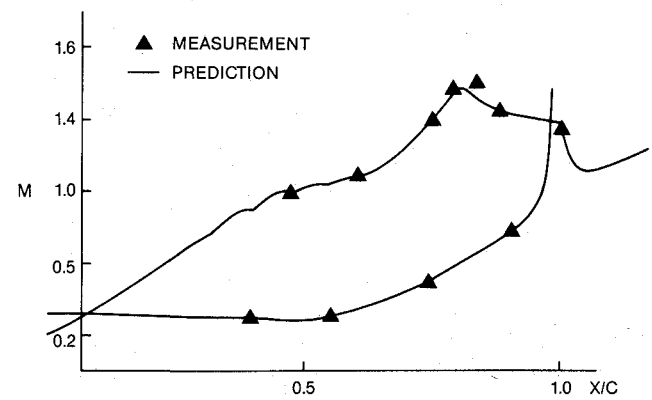

Fig. 5 Comparison of static pressure distribution on blade surface.

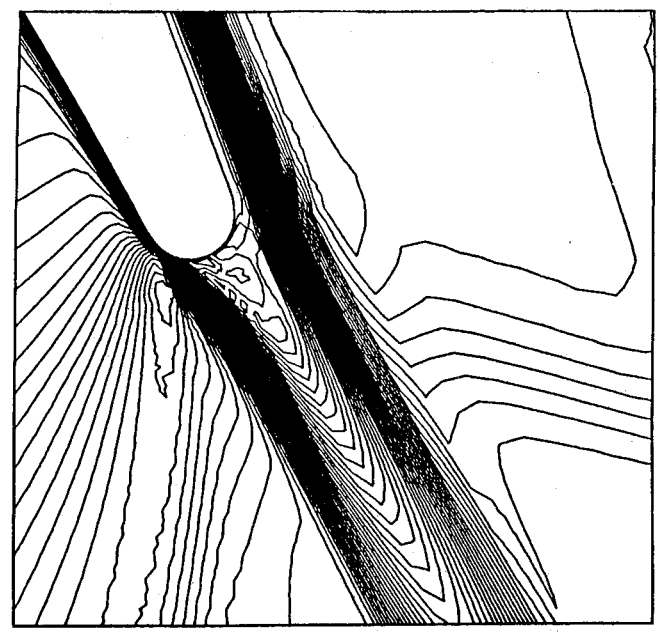

Fig. 6 Calculated Mach number contours near the trailing edge.

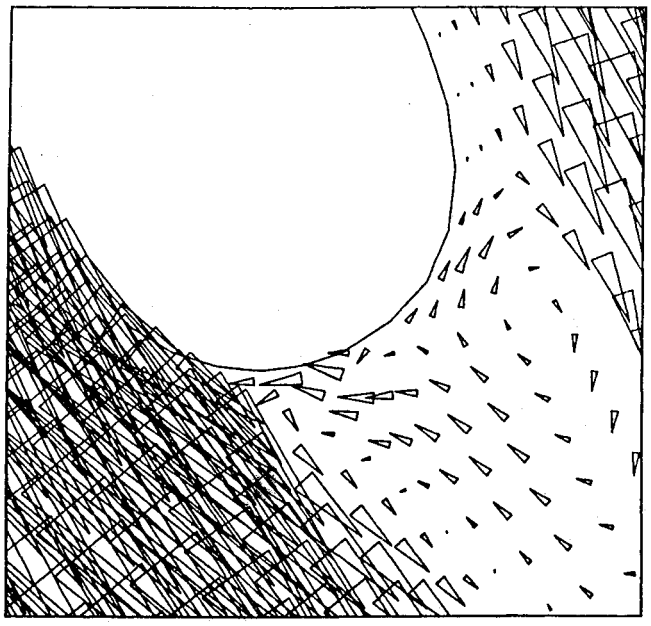

Fig. 7 Calculated velocity vectors near the trailing edge.

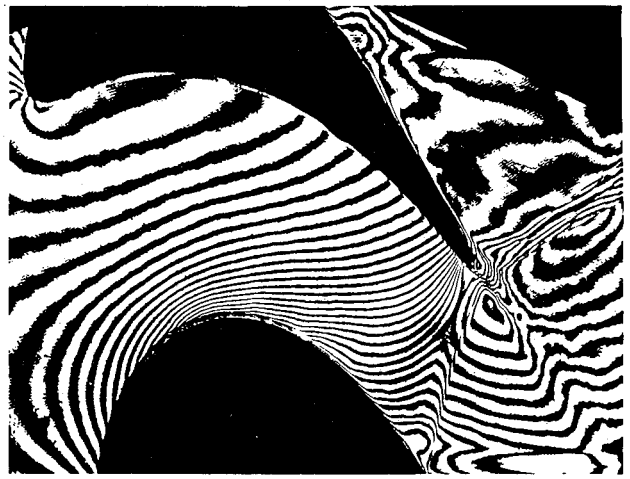

Fig. 8a Measured density contours.

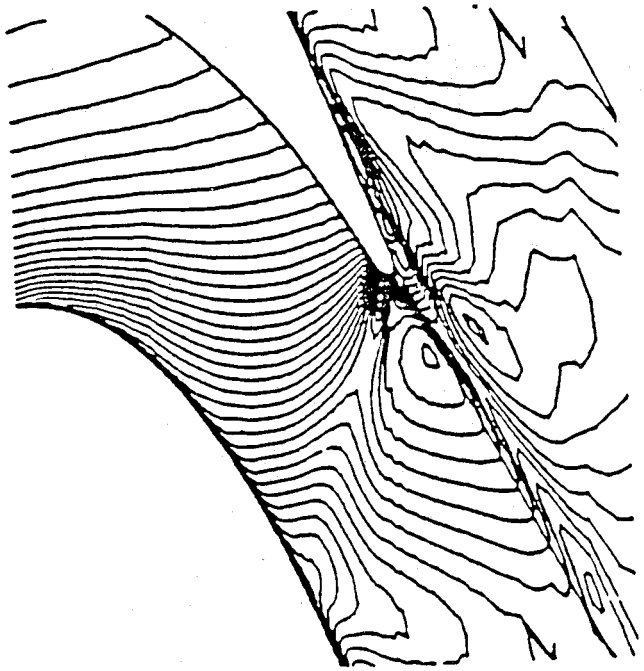

Fig. 8b Density contours from Dawes' calculation.

merical solutions by Dawes[11] and Moore and Moore.[12] The numerical solution by Dawes is based on a time-marching technique with the Baldwin and Lomax turbulence model. The numerical solution by Moore and Moore is based on a pressure-correction method with a simple mixing-length turbulence model. All three numerical solutions predict similar results on the pressure side, where a weak shock interacts with the suction-side boundary layer. However, numerical results on the suction-side shock, which starts just behind the trailing edge and travels toward the next blade row, are very different. The results in Figs. 8b and 8c (from Dawes and Moore and Moore, respectively) indicate that the shock starts

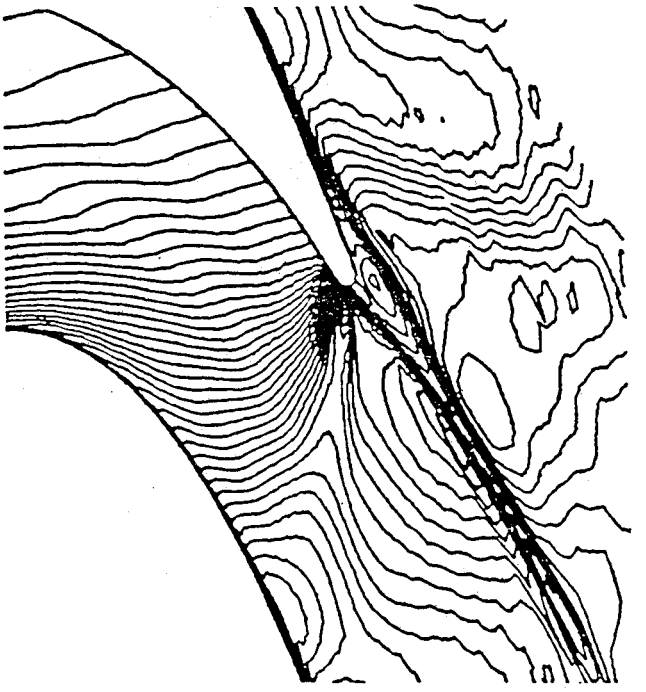

Fig. 8c Density contours from Moore and Moore's calculation.

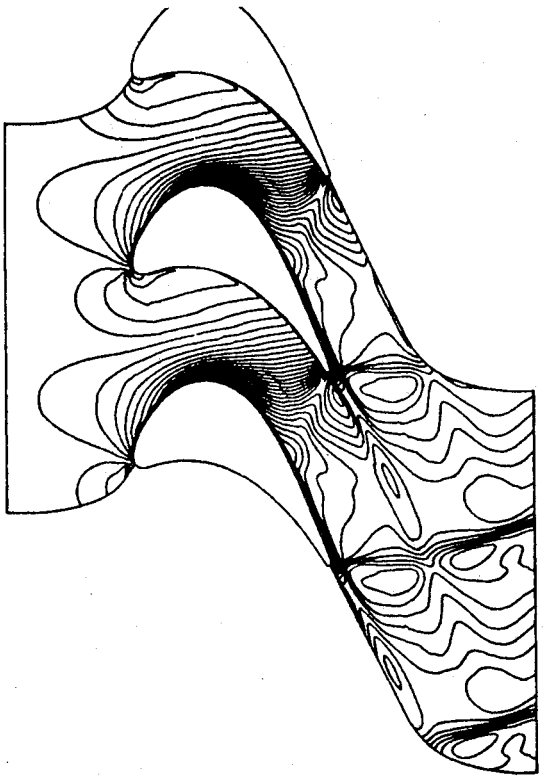

Fig. 8d Density contours from present calculation.

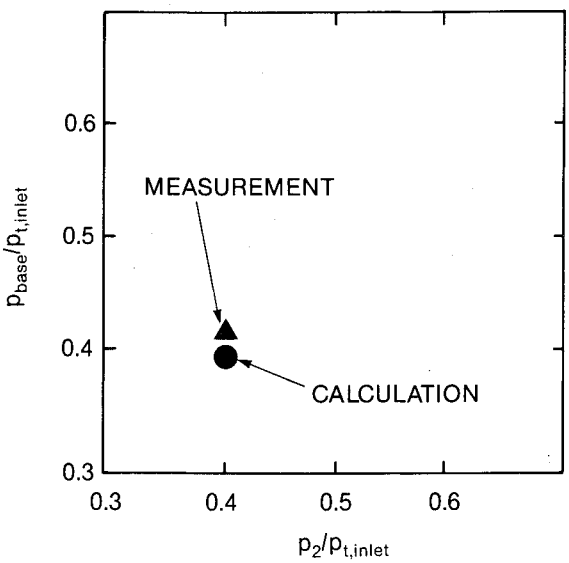

Fig. 9 Comparison of base pressure.

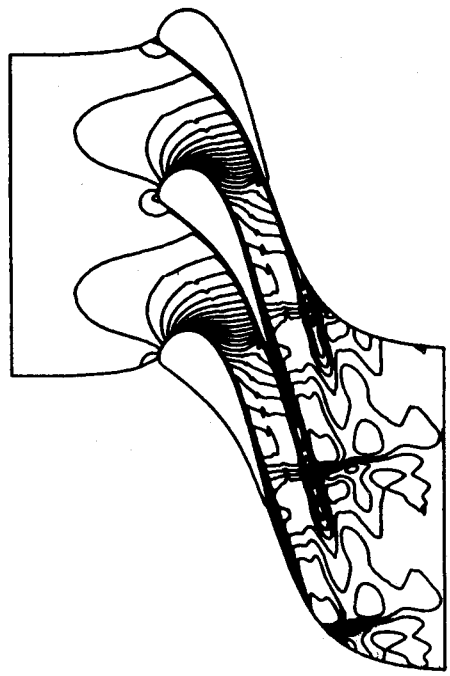

Fig. 10a Calculated Mach number contours (VKI blade).

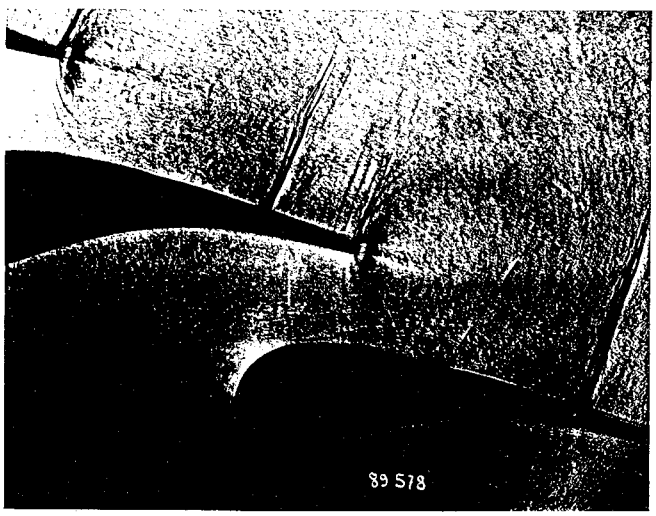

Fig. 10b Photograph of the flow field (VKI blade).

before the trailing edge and the shock strength is almost negligible. The current solution (Fig. 8d) and the interferogram (Fig. 8a) show good agreement and the shock strengths appear to be comparable. Correct and accurate prediction of the trailing edge shock system is critical for the practical design application because of blade interaction in an HP turbine stage. As shown in Fig. 8, proper modeling of viscous stresses and sufficient grid size are required to capture the proper flow physics in transonic turbine flows.

As expected from the calculated density contours on the suction side, the shock induces blade boundary layer separation on the suction side. It is interesting to observe that all three computations indicate flow separation on the suction side, although a quite different shock system is predicted. In Fig. 9, the predicted and measured base pressures are compared, and again, the predicted result agrees very well with the measurement.

VKI Turbine

The current method was also applied to calculate flow and heat transfer in a highly loaded transonic turbine guide vane which was designed and tested at the von Karman Institute (VKI).[13] The experimental data were obtained to verify numerical methods during the 1989 VKI lecture series.

The numerical solution was obtained with a computational grid of 20,400 nodes. Calculated Mach number contours are given in Fig. 10 along with the Schlieren picture of the flow. Unlike the previous two results, the flowfield shows only one shock system on the suction surface because of the lower exit Mach number. The numerical solution captures the overall flowfield very well. As the measurement indicates, the shock disappears after passing through the wake and a rather uniform pressure field is formed downstream. On the suction surface near the trailing edge, the calculated boundary layer looks thicker than the measurement, which results in a rather diffused shock leg. This might be due to the incorrect location of flow transition and requires further study. Detailed velocity vectors near the trailing edge are given in Fig. 11.

Compared with the previous case, the flow is fully attached on the blade suction surface and the typical separation bubble is formed after the trailing edge. For this case, the heat transfer coefficient on the blade surface was calculated and the results are compared in Fig. 12. The overall distribution of heat transfer on the blade surface is quite good. The calculation predicts a somewhat lower heat flux on the pressure

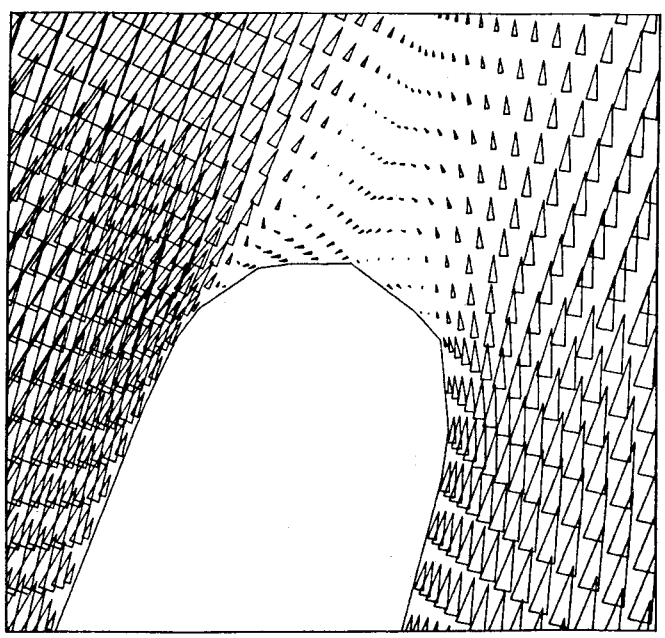

Fig. 11 Detailed velocity vectors near the trailing edge (VKI blade).

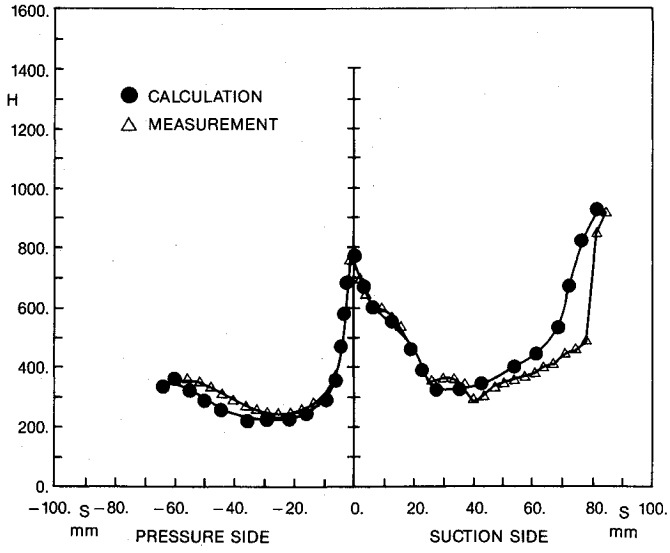

Fig. 12 Comparison of blade surface heat transfer.

side. On the suction side of the blade, the present method predicts flow transition earlier than the measurements, and consequently, higher heat flux is predicted toward the trailing edge. This trend is typical for the current two-equation turbulence model with low Reynolds modification when the free stream turbulence is below 1 to 2%.

Conclusion

A detailed numerical study of the flow and heat transfer inside high-pressure-ratio transonic turbine blade rows was conducted. A high-order upwinding relaxation method with a low Reynolds number version of a two-equation turbulence model was used for the numerical solution. Detailed examination of the numerical solutions for three different turbine sections indicates that the current method predicts very complex flow phenomena near the trailing edge very well. The current method can be applied to the development of advanced HP turbine sections. Further improvement of flow modeling (especially flow transition at low free-stream turbulence level) will enhance the accuracy of the solution.

References

[1]Moore, J., and Moore, J. G., "Performance Evaluation of Linear Turbine Cascades Using Three-Dimensional Viscous Flow Calculations," ASME Paper 85-GT-65, 1985.

[2]Hah, C., "A Navier-Stokes Analysis of Three-Dimensional Turbulent Flows Inside Turbine Blade Rows at Design and Off-Design Conditions," *Journal of Engineering for Gas Turbines and Power*, Vol. 106, 1984, pp. 421–429.

[3]Dawes, W. N., "Development of a 3D Navier-Stokes Solver for Application to all Types of Turbomachinery," ASME Paper 88-GT-70, 1988.

[4]Rhie, C. M., Delaney, R. A., and Mckain, T. F., "Three-Dimensional Viscous Flow Analysis for Centrifugal Impellers," *Journal of Propulsion*, Vol. 1, No. 4, 1985, pp. 257–258.

[5]Denton, J. D., and Xu, L., "The Trailing Edge Loss of Transonic Turbine Blades," ASME Paper 89-GT-278, June 1989.

[6]Sieverding, C. H., Hautot, P., and Decuypere, R., "Investigation of Transonic Steam Turbine Tip Sections with Various Suction Side Blade Curvatures," Institution of Mechanical Engineers, Paper C195/79, 1979.

[7]Hah, C., 1987, "Navier-Stokes Calculation of Three-Dimensional Compressible Flow Across a Cascade of Airfoils With an Implicit Relaxation Method," *AIAA Journal of Propulsion and Power*, Vol. 3, No. 5, pp. 415–422.

[8]Chien, K. Y., "Predictions of Channel and Boundary-Layer Flows With a Low-Reynolds Number Turbulence Model," *AIAA Journal*, Vol. 20, No. 1, 1982, pp. 33–38.

[9]Rodi, W., and Scheuerer, G., "Calculation of Heat Transfer to Convection-Cooled Gas Turbine Blades," *Journal of Engineering for Gas Turbines and Power*, Vol. 107, pp. 620–627, July 1985.

[10]Haller, B. R., "The Effects of Film Cooling Upon the Aerodynamic Performance of Transonic Turbine Blades," PhD Thesis, Cambridge University, Cambridge, England, 1980.

[11]Dawes, W. N., Camus, J-J, Xu, L. P., and Graham, C. G., "Measured and Predicted Loss Generation in Transonic Turbine Blading," AGARD Conference Proceedings No. 401 on Transonic and Supersonic Phenomena in Turbomachines, Munich, West Germany, September 1986.

[12]Moore, J., and Moore, J. G., "Shock Capturing and Loss Prediction for Transonic Turbine Blades Using a Pressure Correction Method," ISABE Proceedings, Paper 89-7017, September 1989.

[13]Sieverding, C. H., private communication.